

## Non-modal stability analysis of a non-Newtonian fluid model

Andrea Tripodi

### 1 Introduction

The growing interest in non-Newtonian fluids is due to the many applications at low-Reynolds number like the microfluidics in biochemistry applications. For example, Newtonian fluids typically flow in the laminar regime at small Reynolds number and mixing occurs via diffusion, an inefficient and slow mechanism. Non-Newtonian fluids can have an advantage with respect to Newtonian fluids for the possibility to generate mixing via purely elastic instabilities and turbulence.

The aim of this project is to support the recent studies done by Boi, Mazzino and Pralits in “Order-disorder transition induces network instabilities in non-Newtonian parallel flows”. In this project we have studied the non-modal stability with optimal disturbances technique of a rheopectic non-Newtonian fluid flow to show the existence of a general mechanism for non-Newtonian instabilities occurring close to zero Reynolds number.

The problem of optimal disturbances, in the context of bypass transition to turbulence, has been of great interest because there are many applications where transition to turbulence occurs without exponential growth, but where there is great potential for transient growth of the disturbance energy in flows that are stable to wave-like perturbations.

### 2 Problem formulation

According to the studies of Boi, Mazzino and Pralits, the non-Newtonian character of the fluid has been described by the following relationship:

$$\mu = \mu_\infty + (\mu_0 - \mu_\infty) (1 + 2a^2\dot{\gamma}^2)^{\frac{n-1}{2}} \quad (1)$$

a widely accepted model to describe the dependence on shear rate of apparent viscosity called Carreau-Bird model. Here  $\dot{\gamma}$  is the strain rate,  $a$  is a constant and  $n$  describe the class of fluid ( $n < 1$  for shear-thinning fluid,  $n > 1$  for shear-thickening fluid,  $n = 1$  for Newtonian fluid). The parameter  $\mu_0$  is the viscosity at zero shear rate (i.e. for  $\dot{\gamma} \rightarrow 0$ ) and  $\mu_\infty$  is the infinite-shear-rate viscosity (i.e.  $\dot{\gamma} \rightarrow \infty$ ). In many case the infinite shear viscosity  $\mu_\infty$  is negligible and the model simplifies.

Following the model introduce in [1], we now introduce an index of fluid finite time response to shear  $\lambda$ . The governing equation of  $\lambda$  come from the requirement the eq. 1, with the simplification of  $\mu_\infty$ , must be obtained in the limit of a fast network response and assume the following relationship:

$$\frac{d\lambda}{dt} = -\frac{\lambda}{\tau} + \frac{2a^2\dot{\gamma}^2}{\tau}$$

where  $d\lambda/dt$  is a material derivative and  $\tau$  is a characteristic time.

To close the circle it is necessary to assume a relation between the time response ( $\lambda$ ) and the fluid ( $\mu$ )

$$\mu = \mu_0 (1 + \lambda)^{\frac{n-1}{2}}$$

The previous parameters are re-sum in some important dimensionless parameters that enter into play: the Reynolds number ( $Re = \rho VL/\mu_0$ ), the Deborah number ( $De = \tau V/L$ ) used to characterize the fluidity of materials and  $\Gamma = aV/L$  that is a measure of the level of how non-Newtonian a fluid is.

We consider a disturbance which behave as

$$\tilde{q}(x, y, z, t) = q(y, t) e^{i(\alpha x + \beta z)}$$

that excite the Kolmogorov parallel flow, here assumed in its two-dimensional form  $U(y) = V \cos(y/L)$ .

We are interested in finding initial optimal disturbances, that is the initial condition that is able to produce the maximum value of an objective function. Our choice of target function is the maximum amplification of final kinetic energy compared to its initial size optimized over all possible initial conditions, commonly called “gain”:

$$G(T) = \frac{E(T)}{E(0)} = \frac{\|\Phi_{out}\|_2^2}{\|\Phi_{in}\|_2^2}$$

### 3 Optimization system

Once the objective function has been identified, the Lagrangian multiplier technique is employed in order to solve the constrained optimization problem.

Since the state of fluid is describe from  $\Phi = (u, v, w, p, \lambda)$  and we want to evaluate the kinetic energy, we define two linear operator to select the velocity components to calculate the energy

$$M_1 : \Phi_{in} \rightarrow \Phi_0 \ \& \ M_2 : \Phi_T \rightarrow \Phi_{out}$$

$$M_1 = \begin{bmatrix} 1 & 0 & 0 \\ 0 & 1 & 0 \\ 0 & 0 & 1 \\ 0 & 0 & 0 \\ 0 & 0 & 0 \end{bmatrix} \ \& \ M_2 = \begin{bmatrix} 1 & 0 & 0 & 0 & 0 \\ 0 & 1 & 0 & 0 & 0 \\ 0 & 0 & 1 & 0 & 0 \end{bmatrix}$$

Using the Lagrange multiplier, we minimize  $J$  as the inverse of  $G$  for all given initial condition  $\Phi_{in}$

$$\min_{\forall \Phi_{in}} J = \frac{1}{G}$$

So the Lagrangian becomes

$$\mathcal{L} = \frac{\|\Phi_{in}\|_2^2}{\|M_2 \Phi_T\|_2^2} - \int_0^T \underline{a}^H \left( \underline{B} \frac{\partial \Phi}{\partial t} + \underline{A} \Phi \right) dt - \underline{b}^H \left[ \Phi_0 - \underline{M}_1 \Phi_{in} \right]$$

where matrices  $A$  and  $B$  contain the expression of the continuity equation, the momentum equation along x, y and z and the lambda equation.

Linearizing and recollecting term, the optimality system becomes:

$$\begin{cases} \underline{B} \frac{\partial \Phi}{\partial t} + \underline{A} \Phi = 0, \ \Phi_0 = \underline{M}_1 \Phi_{in} & \text{direct system} \\ -\underline{B}^H \frac{\partial a}{\partial t} + \underline{A}^H a = 0, \ a(T) = -2 \left( \underline{B}^H \right)^{-1} \underline{M}_2^H \Phi_{out} \frac{\|\Phi_{in}\|_2^2}{\|\Phi_{out}\|_2^2} & \text{adjoint system} \\ \Phi_{in} = -\underline{M}_1^H \underline{B}^H a(0) \frac{\|\Phi_{out}\|_2^2}{2} & \text{optimality condition} \end{cases}$$

The Optimization system has been resolved numerically, so it has been discretized in space and time. A finite difference discretization scheme has been implemented to numerically solve the equations with boundary conditions. The discretization in space is hidden in the definition of matrices  $A$  and  $B$ , while for the discretization in time we use the implicit Euler method. Then, the direct system can be rewritten as

$$\underline{B} \frac{\Phi^{n+1} - \Phi^n}{\Delta t} + \underline{A} \Phi^{n+1} = 0$$

$$\underbrace{\left[ \underline{B} + \Delta t \underline{A} \right]}_{\underline{L}} \Phi^{n+1} = \underline{B} \Phi^n$$

that lead to the solution:

$$\Phi^{n+1} = \underline{L}^{-1} \underline{B} \Phi^n$$

whit initial condition  $\Phi_0 = \underline{M}_1 \Phi_{in}$ .

Similarly, the adjoint equation can be rewrite as

$$\underline{L}^H a^{n+1} = \underline{B}^H a^n$$

with the solution

$$a^n = \left( \underline{\underline{L^H}} \right)^{-1} \underline{\underline{B^H}} a^{n+1}$$

and the initial condition

$$a(T) = -2 \left( \underline{\underline{B^H}} \right)^{-1} \underline{\underline{M_2^H}} \underline{\underline{M_2}} \Phi_T \frac{\|\Phi_{in}\|_2^2}{\|\underline{\underline{M_2}} \Phi_T\|_2^2} = -2 \left( \underline{\underline{B^H}} \right)^{-1} \underline{\underline{M_2^H}} \underline{\underline{M_2}} \Phi_T \frac{J}{\|\underline{\underline{M_2}} \Phi_T\|_2}$$

## 4 Result

Following to the result obtain by Boi, Mazzino and Pralits in “Order-disorder transition induces network instabilities in non-Newtonian parallel flows”, we decide to limit our studies to case with  $\Gamma = De$  and look at four stable case, two unstable case and two Newtonian case as presented in figure 1 and in the table 1.

$Re$	$\Gamma = De$	$n$	Case
0.1	1, 3	1.3	Stable
1	1, 3	1.3	Stable
2	1, 3	1.3	Unstable
1, 2	0.001	1.01	Newtonian

Table 1: Summary of simulations

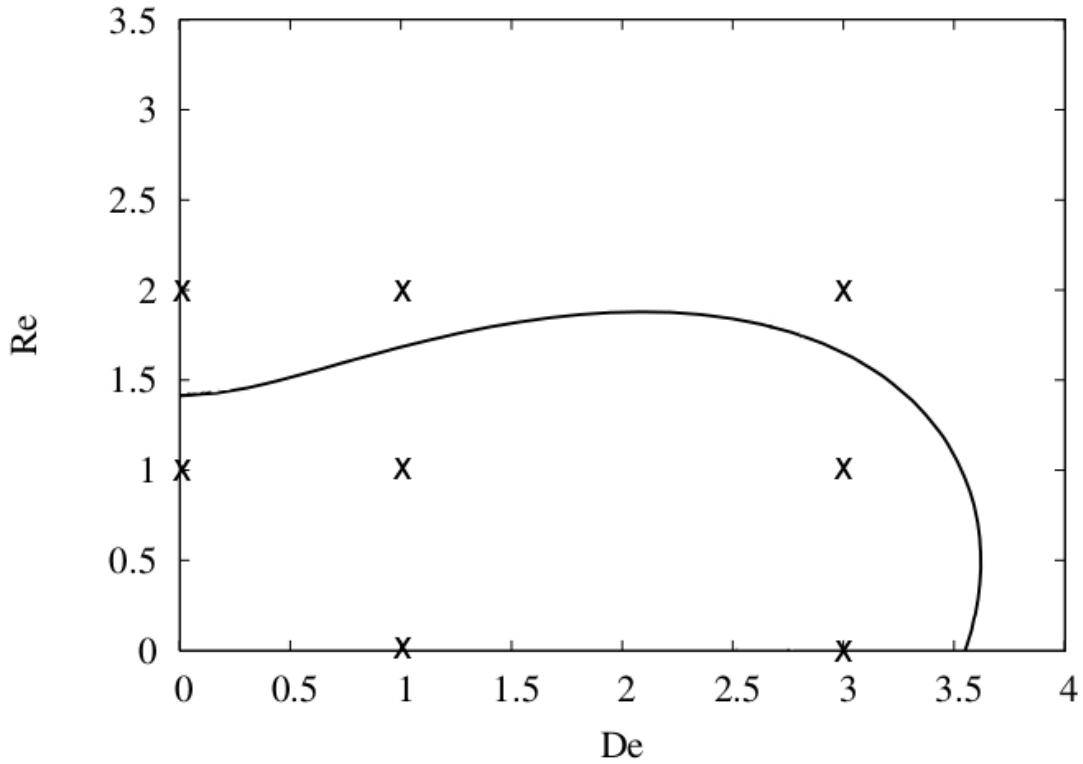


Figure 1: Marginal curve in the  $Re - De$  plane with  $\Gamma = De$  and  $n = 1.3$  and position of simulation done (X)

Below are presented the “gain” trend over time subdivided by type of fluid; blue lines represents the gain trend of a specific time optimization ( $T = 1, 3, 6, 9, 12, 15$ ) while the red one is the envelope of all curves.

- $Re = 0.1, \Gamma = De = 1, n = 1.3$

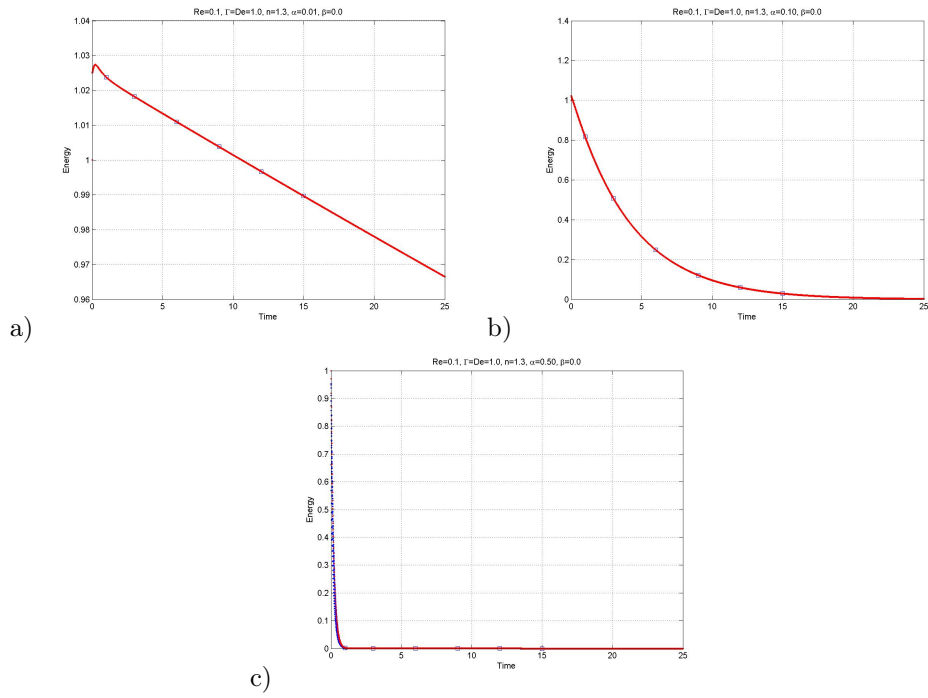


Figure 2: Optimization at different time (blue line) and envelope (red line) of the “gain” trend over time,  $\alpha = 0.01$  (a),  $0.1$  (b),  $0.5$  (c)

- $Re = 0.1, \Gamma = De = 3, n = 1.3$

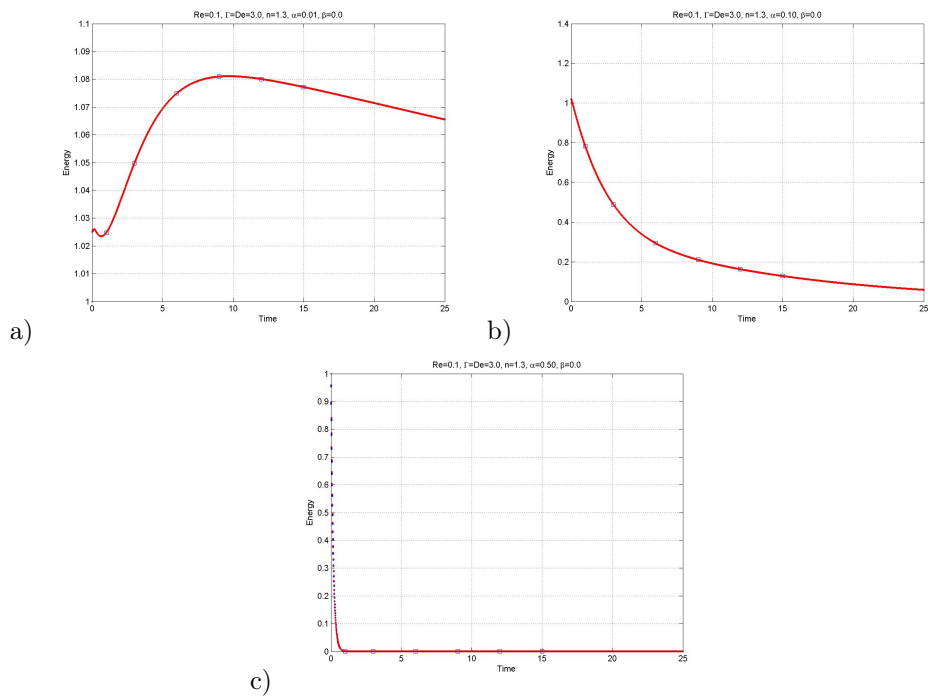


Figure 3: Optimization at different time (blue line) and envelope (red line) of the “gain” trend over time,  $\alpha = 0.01$  (a),  $0.1$  (b),  $0.5$  (c)

- $Re = 1, \Gamma = De = 1, n = 1.3$

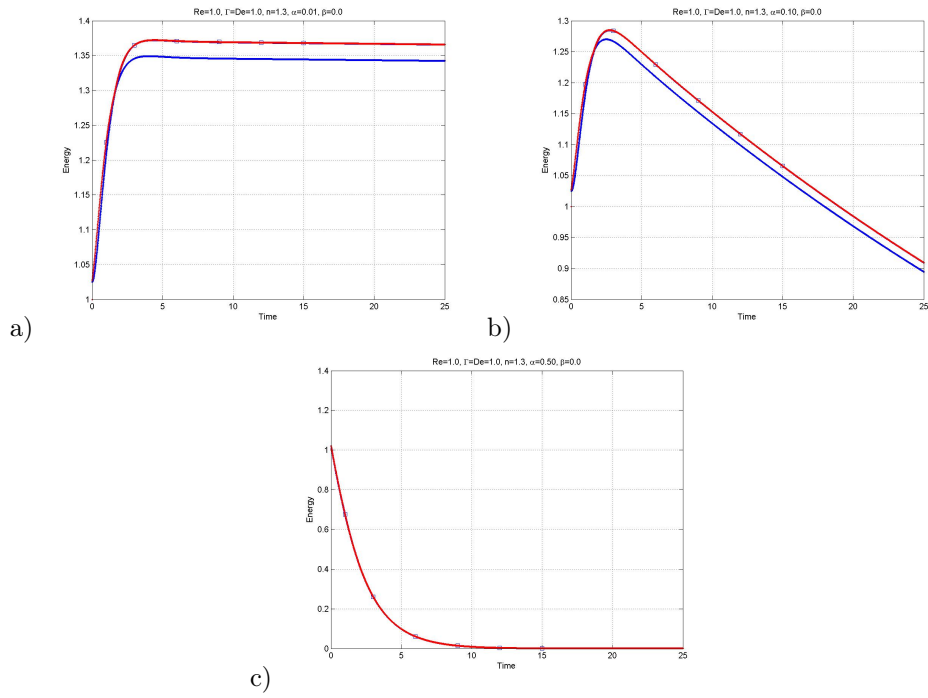


Figure 4: Optimization at different time (blue line) and envelope (red line) of the “gain” trend over time,  $\alpha = 0.01$  (a),  $0.1$  (b),  $0.5$  (c)

- $Re = 1, \Gamma = De = 3, n = 1.3$

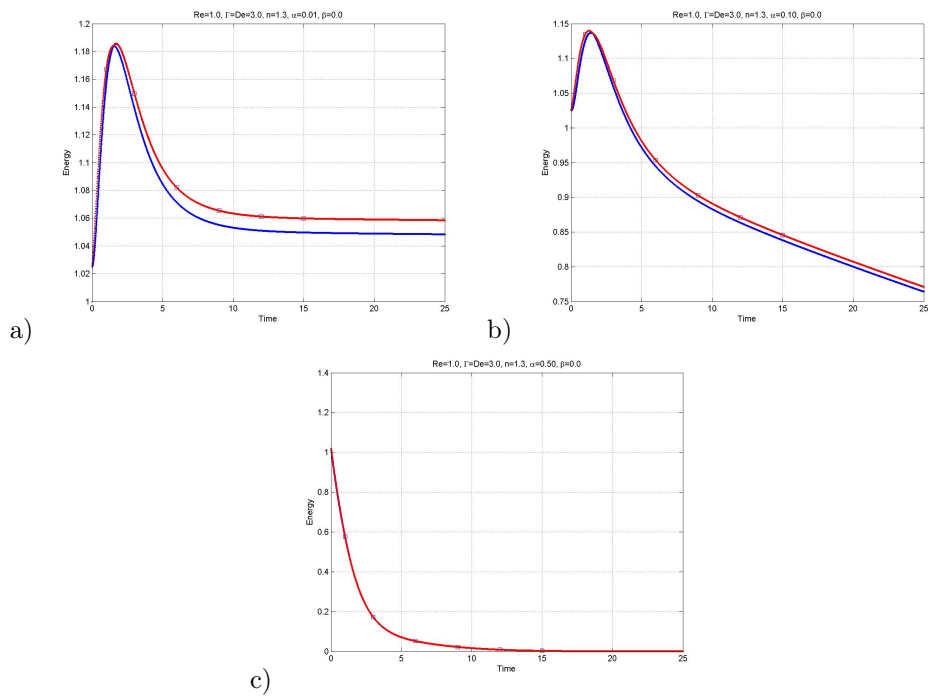


Figure 5: Optimization at different time (blue line) and envelope (red line) of the “gain” trend over time,  $\alpha = 0.01$  (a),  $0.1$  (b),  $0.5$  (c)

- $Re = 2, \Gamma = De = 1, n = 1.3$

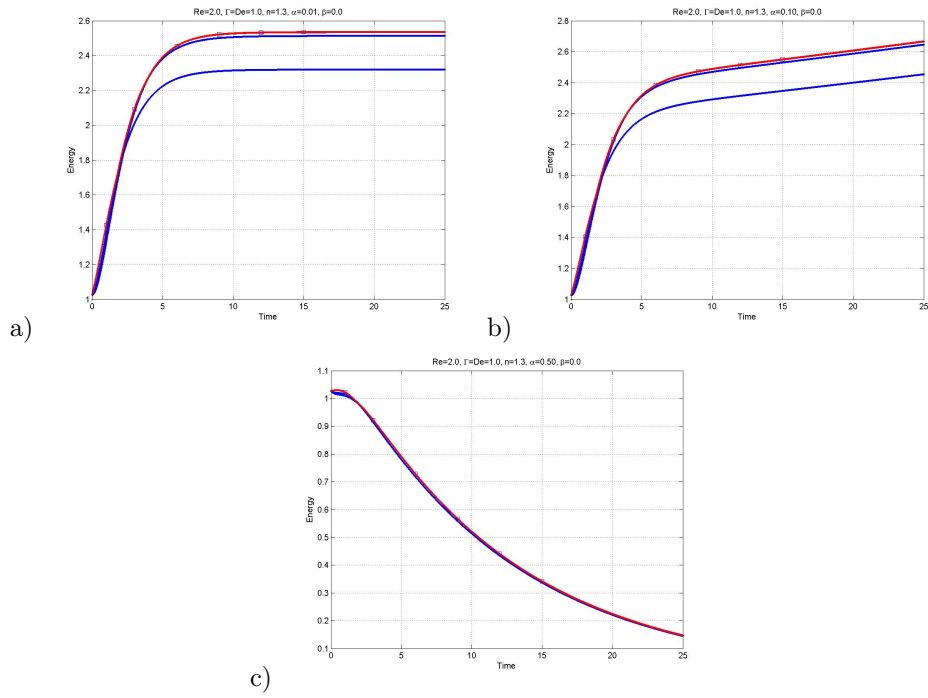


Figure 6: Optimization at different time (blue line) and envelope (red line) of the “gain” trend over time,  $\alpha = 0.01$  (a),  $0.1$  (b),  $0.5$  (c)

- $Re = 2, \Gamma = De = 3, n = 1.3$

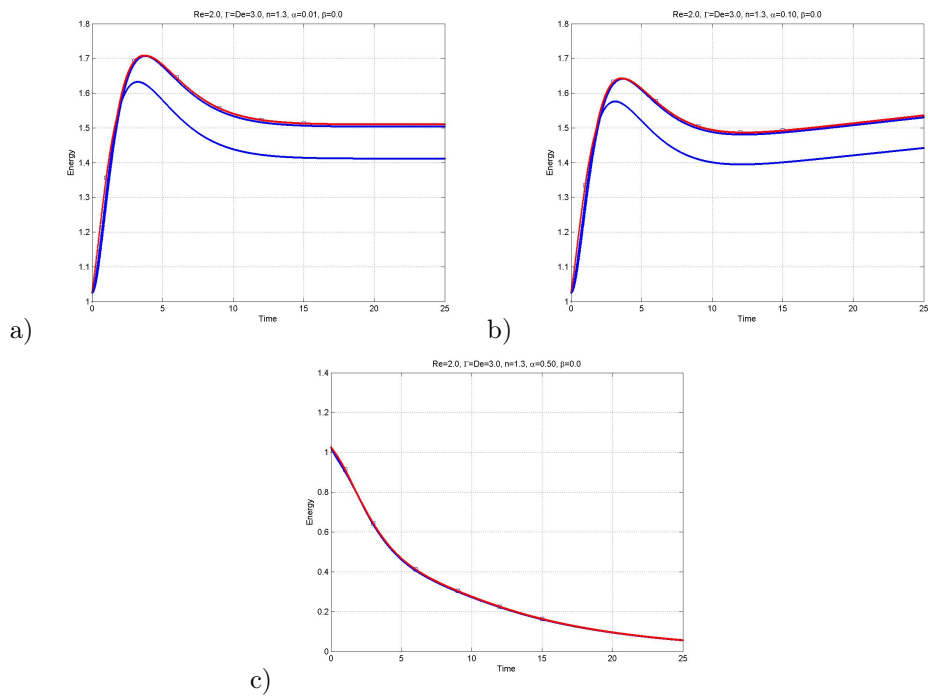


Figure 7: Optimization at different time (blue line) and envelope (red line) of the “gain” trend over time,  $\alpha = 0.01$  (a),  $0.1$  (b),  $0.5$  (c)

- *Newtonian* :  $Re = 1$ ,  $\Gamma = De = 10^{-3}$ ,  $n = 1.01$

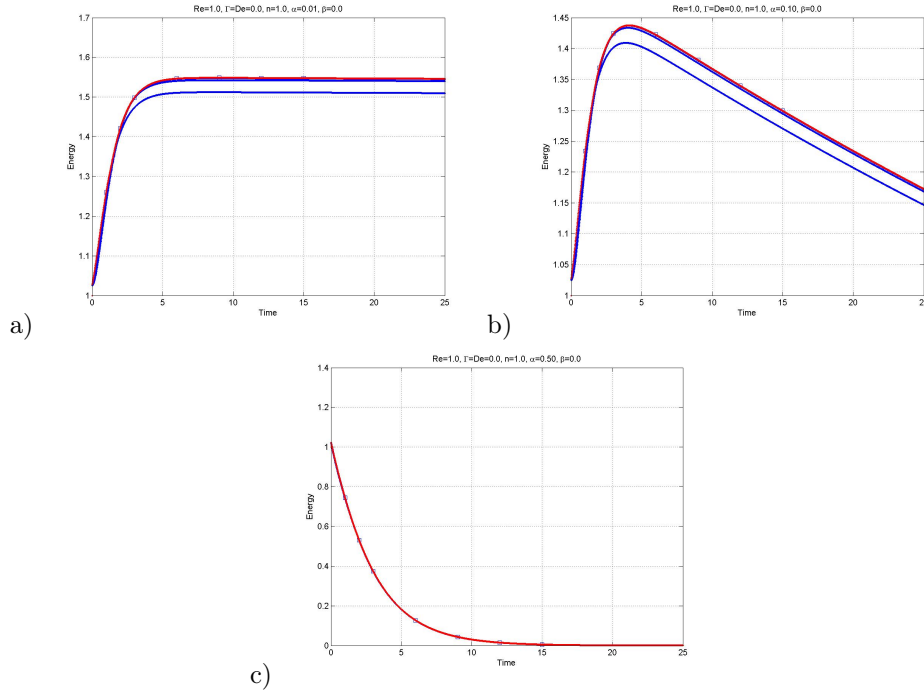


Figure 8: Optimization at different time (blue line) and envelope (red line) of the “gain” trend over time,  $\alpha = 0.01$  (a), 0.1 (b), 0.5 (c)

- *Newtonian* :  $Re = 2$ ,  $\Gamma = De = 10^{-3}$ ,  $n = 1.01$

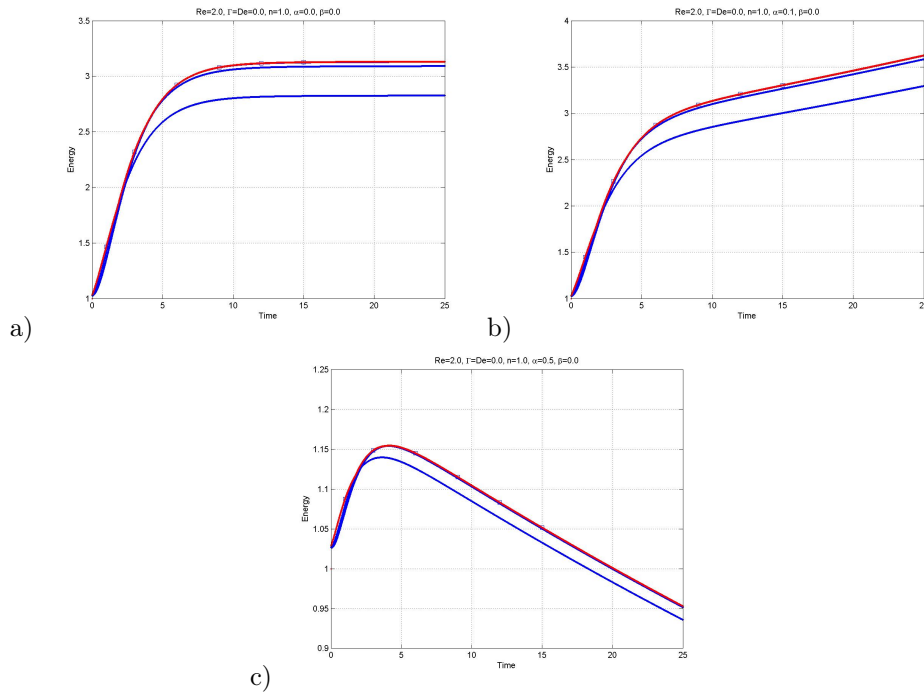


Figure 9: Optimization at different time (blue line) and envelope (red line) of the “gain” trend over time,  $\alpha = 0.01$  (a), 0.1 (b), 0.5 (c)

Below, will be presented the summary graphs subdivided by Reynolds number. For every Reynolds number, the first graph is the trend of the maximum achievable energy over all possible value of  $\alpha$ , while the second graph is the the value of  $\alpha$  corresponding to the maximum energy.

- $Re=0.1$

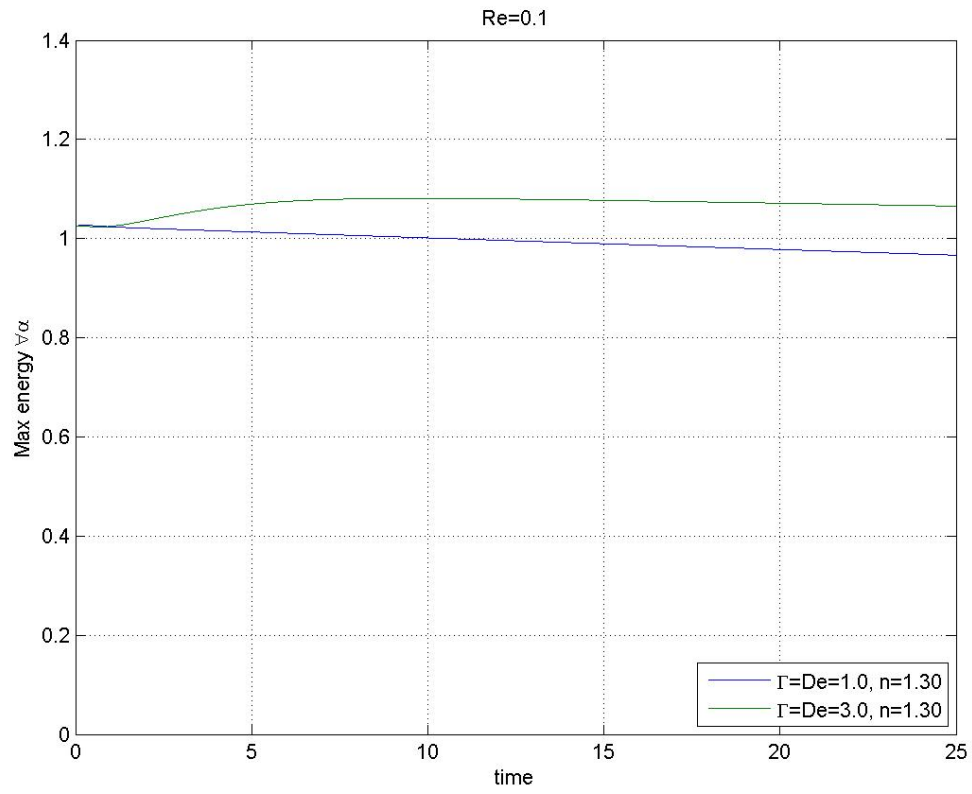


Figure 10: Max energy at every time over all  $\alpha$

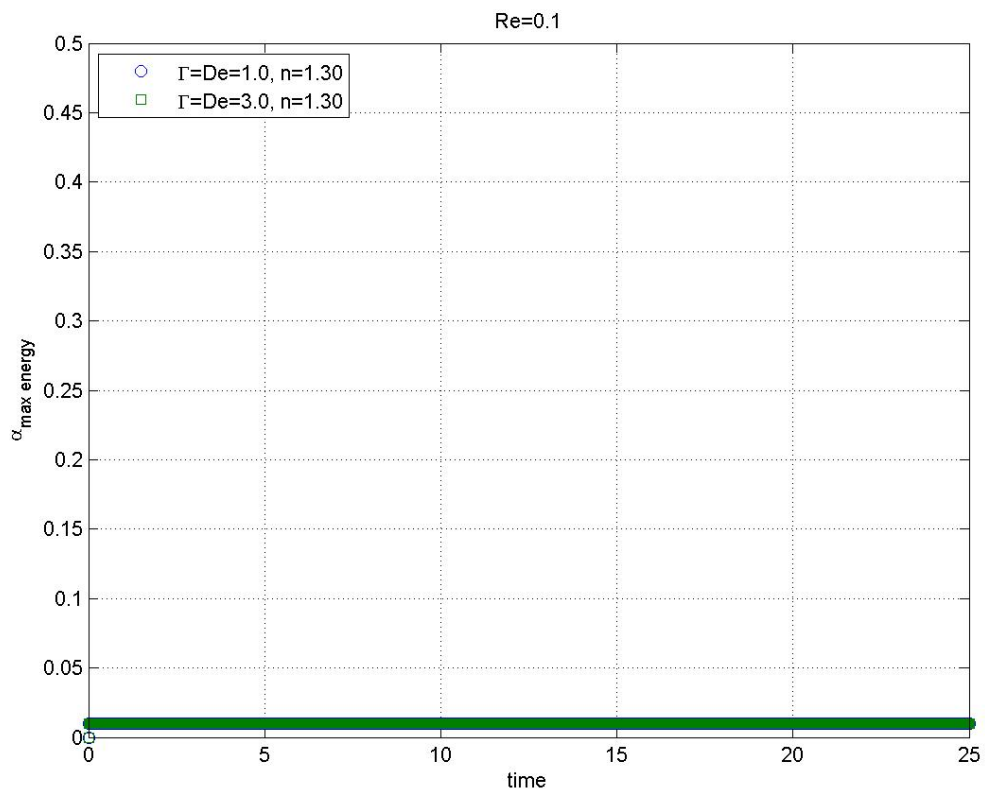


Figure 11: Value of  $\alpha$  of the maximum energy

- $Re=1$

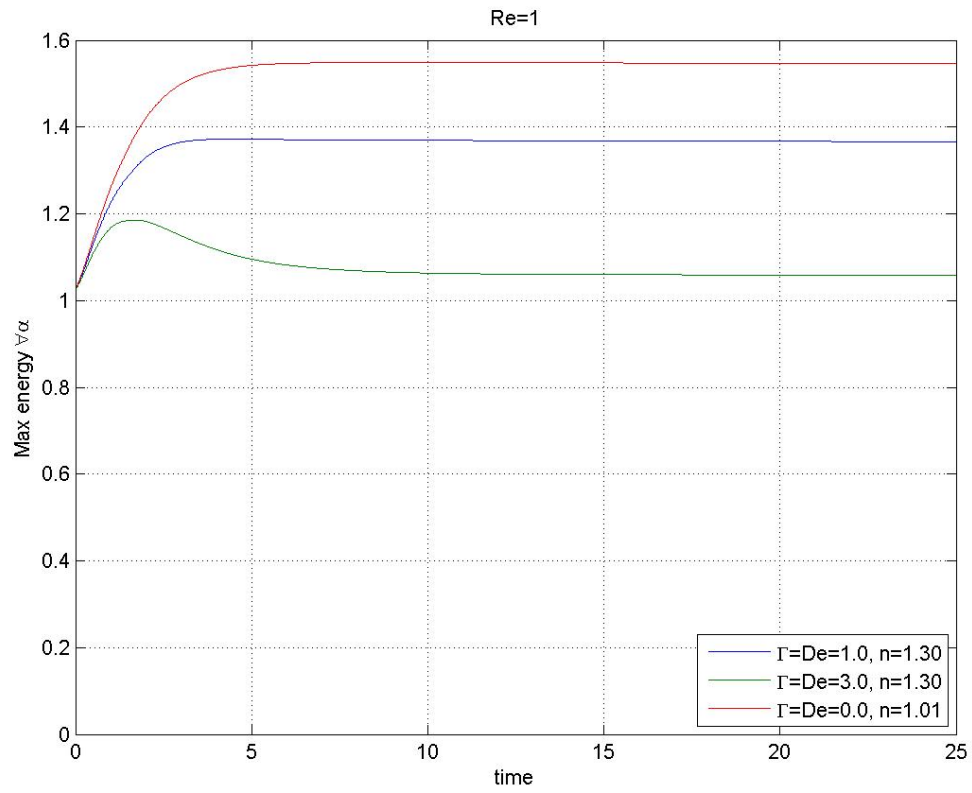


Figure 12: Max energy at every time over all  $\alpha$

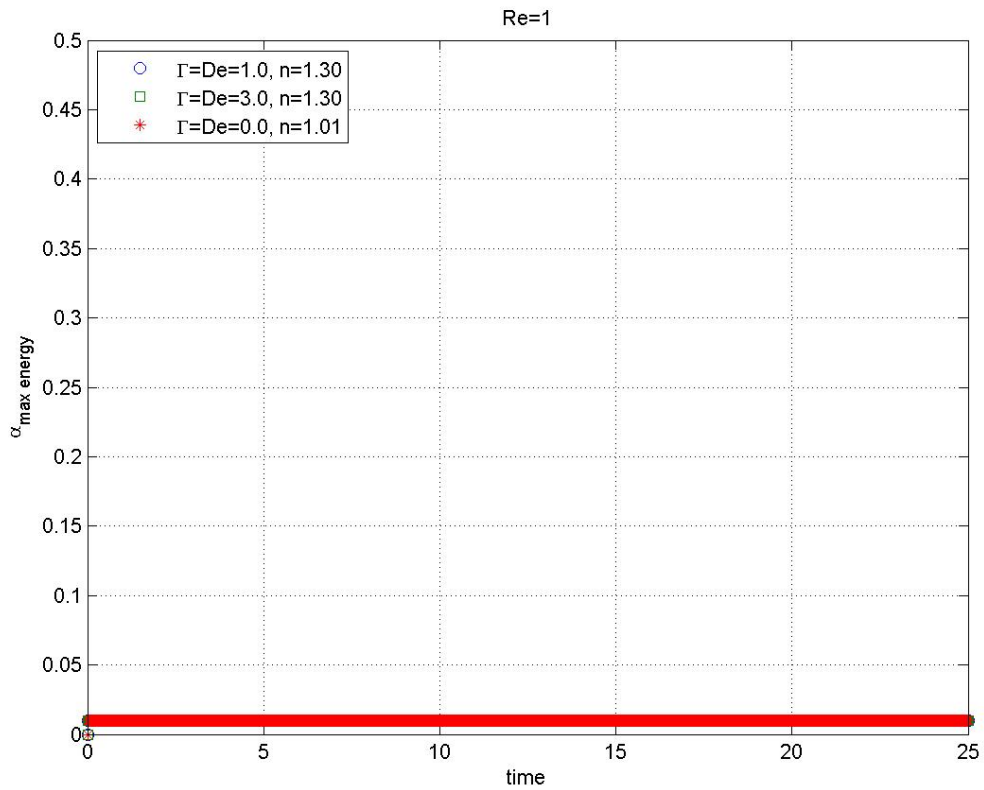


Figure 13: Value of  $\alpha$  of the maximum energy

- Re=2

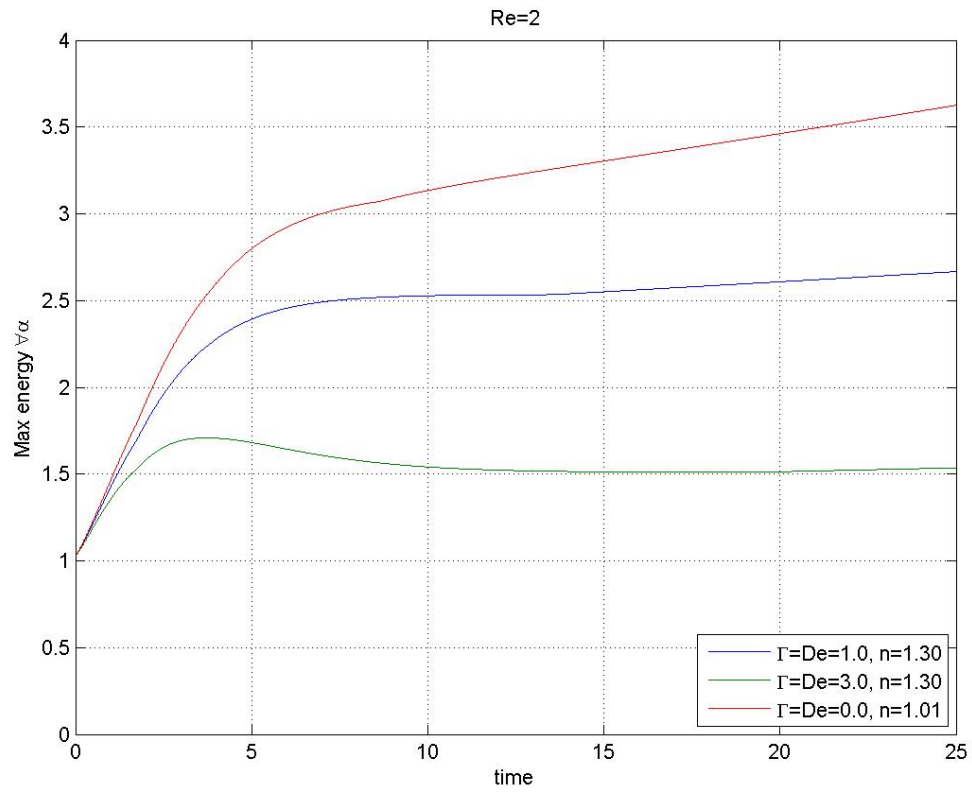


Figure 14: Max energy at every time over all  $\alpha$

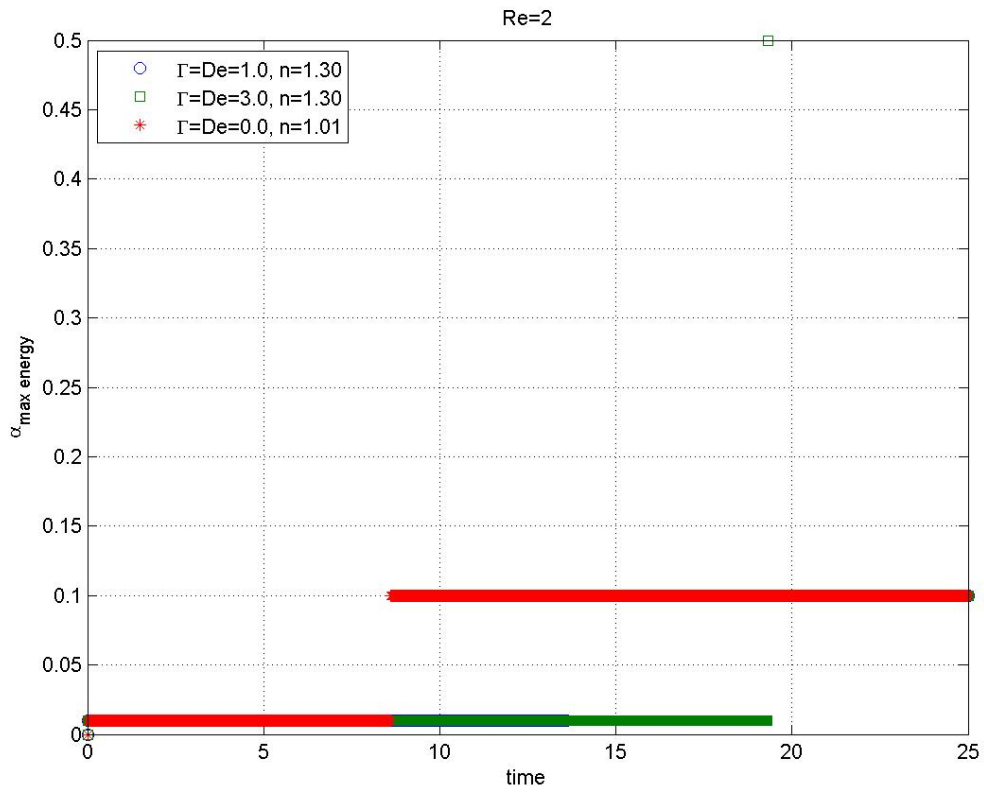


Figure 15: Value of  $\alpha$  of the maximum energy

## 5 Conclusion

In this project has been investigated the transient growth of a model of non-Newtonian fluid to support recent studies [1].

The main result is the identification of an almost similar response to perturbation between non-Newtonian and Newtonian model. Similar result has been reached in [2] with simulation on the same model with a flow in a channel. Figures 10, 12 and 14 represent the trend of gain function and they shows that different types of fluid share an almost similar behavior.

Another common behavior is the tendency to stabilize increasing the parameter  $\alpha$ . This feature is shown in figures 11, 13 and 15 where is represented the value of  $\alpha$  which correspond the maximum of energy; for every types of fluid the maximum energy has been reached with the minimum value of  $\alpha$  used in ours simulation.

Furthermore, figures of the optimizations show an almost limited transient growth; for stable simulation the energy reach at the peak less than 2 times the initial energy.

## References

- [1] S. Boi, A. Mazzino and J. O. Pralits, “Minimal model for zero-inertia instabilities in shear-dominated non-Newtonian flows”, *Phys. Rev. E*, 88, 033007 (2013)
- [2] M. Zhang, I. Lashgari, T. A. Zaki, Luca Brandt, “Linear stability analysis of channel flow of viscoelastic Oldroyd-B and FENE-P fluids”, *J. Fluid Mech.* (2013, submitted)
- [3] Lecture course Advanced Fluid Dynamics, 2013